

# Low Signal-to-Noise Ratio Radar Target Detection using Linear Support Vector Machines (L-SVM)

John E. Ball

Department of Electrical and Computer Engineering  
Mississippi State University  
Starkville, MS, USA  
jeball@ece.msstate.edu

**Abstract**—This paper examines target detection using a Linear Support Vector Machine (L-SVM). Traditional radars typically use a Constant False Alarm Rate (CFAR) processor to adaptively adjust the detection threshold based on the fast-time return signal. The SVM formulation uses the same block-diagram structure as the CFAR approach; however, data from the leading and lagging windows is directly used to classify each cell under test. The L-SVM method is compared to a Cell-Averaging CFAR (CA-CFAR) on simulated radar return signals with and without Swerling I targets. The results show that the L-SVM is able to detect very small SNR signals, while the CA-CFAR is unable to detect these signals below  $-10$  dB SNR. In addition, the probability of detection and probability of false alarm for the L-SVM degrade much more gracefully than for the CA-CFAR detector for low-SNR targets.

## I. BACKGROUND

Target detection of radar signals is a difficult problem when the Signal-to-Noise Ratio (SNR) is low. Constant False Alarm Rate (CFAR) processors are typically used in radar applications, since they offer control over the false alarm rate as well as adaptability to the environment. CFAR processors are suitable if the target SNR is large enough [1]. However, in scenarios where the target SNR is low, CFAR processing can set the detection threshold high, and will miss low-SNR targets. This paper investigates how a CFAR system block diagram can be modified by using a Linear Support Vector Machine (L-SVM) for target detection.

This paper is organized as follows. Sections I A and B overview CFAR processors and L-SVMs. Section II covers the proposed L-SVM methodology and gives details about the simulation parameters. Section III describes the experiments. Discussion on the results and future work is listed in sections IV and V, respectively.

### A. CFAR Processor

One-dimensional (1D) CFAR algorithms adjust the target detection threshold based on estimated statistics of the leading and lagging windows. The 1D CFAR algorithms examine each range bin and compute a function of the leading and

lagging windows, as shown in fig. 1 [1]. In Cell-Averaging CFAR (CA-CFAR), the functions  $f_1$  and  $f_2$  average the return data in the leading and lagging windows in order to estimate the interference power. The threshold for each cell under test is adaptively adjusted based on the estimated interference power [1]. This process is repeated for each range bin. The guard cells on either side for the cell under test (CUT) allow for targets that span more than one range bin. The CFAR algorithms set a maximum probability of false alarm, while simultaneously achieving a high probability of detection, assuming the target SNR is high enough.

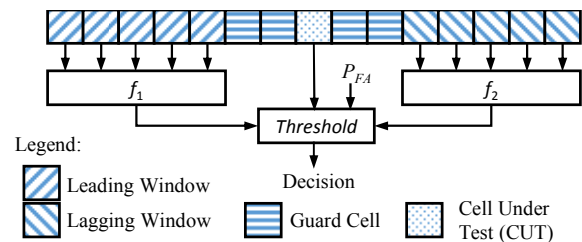


Figure 1. CFAR Processor Architecture.

### B. Support Vector Machines (SVM)

SVMs have been used extensively in classification and pattern recognition applications [2] (see also references in this tutorial). Properly trained SVMs can provide high classification accuracies [2]. SVMs have been used in a CFAR detector scheme for network traffic [3]. Examples of SVM applications in radar include radar pulse classification [4], ocean clutter suppression [5], low-observable target detection in sea clutter using SVM and multifractal correlation [6], and radar target recognition using a two-stage SVM procedure [7].

For this paper, the linear SVM (L-SVM) is utilized. The L-SVM implementation is the LIBLINEAR library [8], which is an extension to the LibSVM library [9]. The L-SVM solves the following unconstrained optimization problem

$$\frac{1}{2} \mathbf{w}^T \mathbf{w} + C \sum_{j=1}^L \xi(\mathbf{w}_j; \mathbf{x}_j, y_j), \quad (1)$$

where  $\mathbf{w} = [w_1, w_2, \dots, w_N]^T$  is the  $[N \times 1]$  optimal weight vector,  $\mathbf{x}_j$  is a  $[N \times 1]$  feature vector,  $y_j \in \{-1, 1\}$  is the class associated with  $\mathbf{x}_j$  (1=target, -1=no target),  $C$  is a penalty parameter for misclassifications, and  $\xi$  is a convex loss function, which allows for well-known convex optimization strategies to be employed in solving for the optimal weight vector, and  $L$  is the number of training samples. The loss function is used in classifier training; it will be near zero when a training sample is correctly classified, and will increase in value based on the distance to the classification boundary if the training sample is incorrectly classified.

In the training phase, target and non-target training data is presented to the L-SVM and the weight is optimized to best discriminate target cases from non-target cases. The target data in this case is simulated, and can also be simulated in a radar since targets may not be present. In the testing phase, new feature vectors are presented and they are considered targets if the L-SVM weighted feature  $z$  is greater than zero,

$$z = \mathbf{w}^T \mathbf{x} > 0 \quad (2)$$

and non-targets otherwise. The L-SVM implementation is very fast and computationally efficient.

## II. METHODOLOGY

A notional S-band volume search radar with parameters shown in Table I was simulated in Matlab<sup>TM</sup>. The radar is assumed to be operating in a low clutter environment. Therefore, the radar return signal will be corrupted with complex white Gaussian noise. A single Linear Frequency Modulated (LFM) chirp pulse is used. The radar returns are from Swerling I targets at various ranges. Each target's RCS is set using the radar equation, based on the desired SNR.

TABLE I. NOTIONAL RADAR PARAMETERS

Parameter	Value	Parameter	Value
Pulse Width	10 $\mu$ s	Guard Cell Size <sup>a</sup>	15 Cells
PRI	1 ms	Antenna Gain (dB)	17.0
Center Frequency	3.0 GHz	System Losses (dB)	4.0
Number of Pulses	1	System Noise Figure (dB)	8.0
Fast-Time Sampling Rate (baseband)	80 MHz	LFM Chirp Time-Bandwidth Product	100
Leading and Lagging Window Size <sup>a</sup>	30 Cells	CFAR $P_{FA}$	$1.0 \times 10^{-5}$

a. The leading and lagging window and the guard cell sizes are the sizes on one side of the cell under test. The total number of window and guard cells will be twice this number.

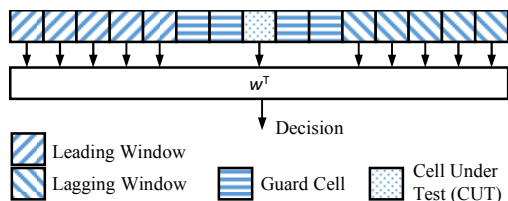


Figure 2. L-SVM Processor Architecture.

The block diagram of the L-SVM method is outlined in fig. 2. Comparing fig. 1 with fig. 2 shows that all of the window data (except the guard cells) is utilized directly in the SVM implementation, vs. the CFAR algorithm, which

provides a scalar output (the estimated interference power) from the window data. The penalty parameter  $C$  was chosen to be 8.0, and the  $L2$  regularized  $L2$ -loss SVM classification scheme was chosen (option “-s 2” in LIBLINEAR *train* function). The loss function is

$$\xi = \max(1 - y_j \mathbf{w}^T \mathbf{x}_j, 0)^2. \quad (3)$$

## III. EXPERIMENTS

To test the L-SVM method, the return signal SNR was varied from -25 to 15 dB, as shown in Table II, below. From Table II, experiment 1 is an easy scenario; both methods should do well. Experiment 2 is a harder scenario, and experiment 3 verifies that high-SNR targets can still be detected when trained on low-SNR targets. Experiments 4 and 5 are very difficult, and experiment 6 spans the entire range of SNR values.

TABLE II. EXPERIMENT DESCRIPTIONS

Exp.	Target SNR	Exp.	Target SNR
1	5 dB	4	-10 dB
2	0 to 15 dB	5	-25 dB
3	0 dB	6	-25 to 15 dB

In each experiment, training data is generated containing with and without targets. In a radar system, target training data can be injected into returns or taken from targets in firm track. Independent testing data was generated and tested via the L-SVM and CFAR methods. The data is complex, and pulse compression using the LFM matched filter is performed prior to applying the detection algorithms.

A qualitative comparison of the Receiver Operating Characteristics (ROC) curves [10] is shown, and the following quantitative methods are used:  $A_Z$ , the area under the ROC curve;  $FP$ , the number of false positives (false alarm); and  $FN$ , the total number of false negatives (misses);  $P_D$ , the probability of detection; and  $P_{FA}$ , the probability of false alarm. ROC  $A_Z$  is a figure of merit for detectors.  $A_Z$  is in  $[0.5, 1.0]$ , and a higher  $A_Z$  usually indicates better performance. For  $FP$  and  $FN$ , lower numbers indicate better performance. However, in general, a small number of false positives is better than missed detections.  $P_D$  and  $P_{FA}$  are estimated based on the test data; the radar should have the highest possible  $P_D$  for a given  $P_{FA}$ .

## IV. RESULTS AND DISCUSSION

Table III shows the results for the experiments. From the table, the L-SVM  $A_Z$  is 1.0 until experiment 4 – 6, and it falls off very gradually even with the very small -25 dB SNR targets in experiment 6. In contrast, the CFAR detector falls off dramatically with experiment 4 (SNR = -10 dB), and is totally unable to detect targets in experiment 5. Both methods achieve a very low percentage of false positives. However, note that the  $P_D$  for the CFAR in experiments 4 and 5 is almost zero. That explains the low percentage of FP for the CFAR: there were almost no detections because the CFAR threshold is too high to detect the low SNR targets. Both methods had no false alarms until experiments 4 and 5. Experiment 5 shows the classic tradeoff in detector

performance: the L-SVM must admit a few more false alarms in order to detect the smaller signals. The L-SVM has a low number of FNs, indicating that most targets were not missed. However, the CFAR detector performance is very poor when the SNR < -10 dB.

TABLE III. EXPERIMENT RESULTS. THE SVM RESULTS ARE SHOWN IN BOLD AND THE CFAR RESULTS UNDERNEATH IN NON-BOLD TEXT.

Exp.	$A_Z$	FP(%)	FN(%)	$P_D^a$	$P_{FA}^a$
1	<b>1.0000</b>	<b>0.0000</b>	<b>0.0000</b>	<b>1.0000</b>	<b>0.0</b>
	1.0000	0.0000	0.0000	1.0000	0.0
2	<b>1.0000</b>	<b>0.0000</b>	<b>0.0000</b>	<b>1.0000</b>	<b>0.0</b>
	0.9979	0.0000	0.0011	0.9978	0.0
3	<b>1.0000</b>	<b>0.0000</b>	<b>0.0000</b>	<b>1.0000</b>	<b>0.0</b>
	0.9867	0.0000	0.0144	0.9717	0.0
4	<b>0.9991</b>	<b>0.0962</b>	<b>0.0007</b>	<b>0.9987</b>	<b>4.9187 e-6</b>
	0.5088	0.0000	0.5015	0.0195	0.0
5	<b>0.9682</b>	<b>4.7115</b>	<b>0.0321</b>	<b>0.9372</b>	<b>2.4140 e-4</b>
	0.5000	0.0000	0.5115	0.0000	0.0
6	<b>0.8140</b>	<b>0.0702</b>	<b>0.2139</b>	<b>0.7909</b>	<b>7.1828 e-5</b>
	0.6200	0.0000	0.5247	0.4872	0.0

a. PD and PFA were estimated based on the test data.

Figs. 3 – 5 show the PDFs of the weighted L-SVM feature vector ( $z$ ) for the non-target and the target cases for experiments 1, 4, and 5. In all cases, the non-target PDF is the curve to the left, while the target PDF is the curve to the right. Even when the SNR is -25 dB, there is very little overlap in the two PDFs, which is why the L-SVM is able to achieve good results. Figs. 6 and 7 show ROC curves for experiments 5 and 6, respectively. From fig. 6, the CFAR detector has  $A_Z = 0.5$ , which indicates it is not able to distinguish targets from the non-targets. The signal is just too low to allow the adaptive threshold to declare a target present.

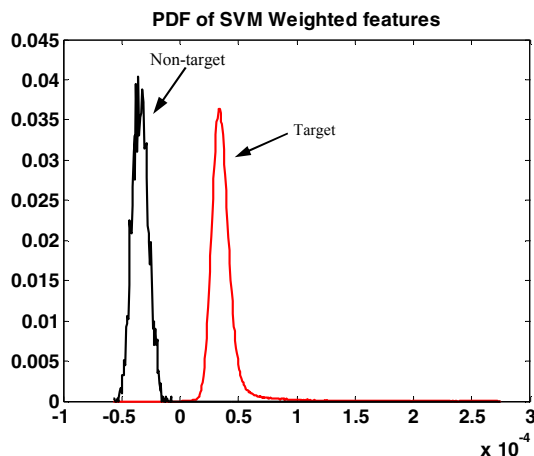


Figure 3. PDF of SVM statistic  $z$  for Experiment 1 (SNR = 5 dB).

Figure 7 shows that when the SNR is high, the two detectors behave similarly. The ROC curve in experiment 6 has many different SNR scenarios, and that is why the curves are flat for most of the plot then take on a 45 degree slope. The upper-right portion of the curve is due to the very low SNR targets that neither detector can handle with one pulse. Note how quickly the ROC curve for the CA-CFAR detector degrades at a very low  $P_{FA}$ , while the L-SVM is able to detect the lower SNR targets. This shows graceful degradation of the

L-SVM. However, the CA-CFAR performs poorly for lower SNR values, and the L-SVM degrades more gracefully.

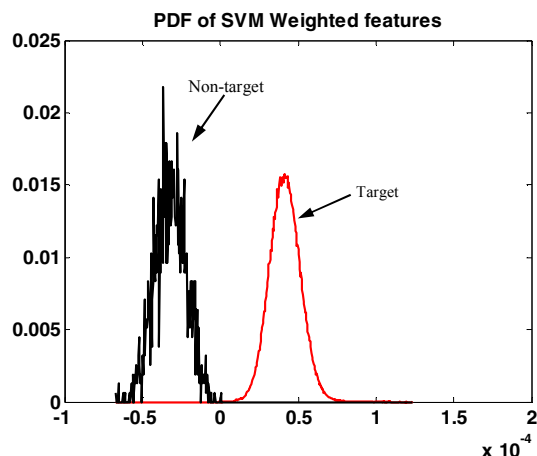


Figure 4. PDF of L-SVM statistic  $z$  for Experiment 4 (SNR = -10 dB).

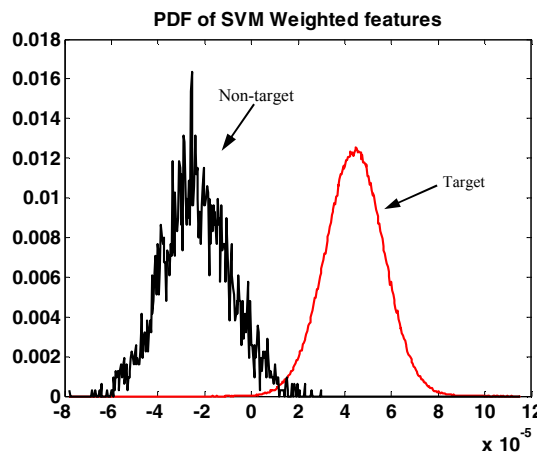


Figure 5. PDF of L-SVM statistic  $z$  for Experiment 5 (SNR = -25 dB).

Fig. 8 shows a segment of the pulse-compressed radar return amplitudes, with the CFAR threshold superimposed. From this figure it is evident that the CFAR threshold is just too high to detect the small SNR targets near indices 500 and 1500. Fig 9 shows a similar segment of the L-SVM feature. The threshold is a constant, zero. Fig. 9 shows two true detections and one false alarm caused by the noise, which happened in this instantiation to add enough to bring the feature over the zero threshold mark.

In conclusion, the L-SVM method shows more graceful degradation for low SNR cases, while the CA-CFAR processor more abruptly fails and stops detecting altogether. The disadvantage of the L-SVM method is that training is required. In benign environments (i.e. Gaussian noise), this is not a problem. In a more dynamic environment where clutter returns dominate (i.e. a Naval horizon search mode, where there is strong sea clutter return), training would be required periodically. This could be done using a listen-only mode; many radars employ this technique to produce clutter maps

and listen for interference sources. Once trained, the target test is simply checking the sign weighted vector in (2).

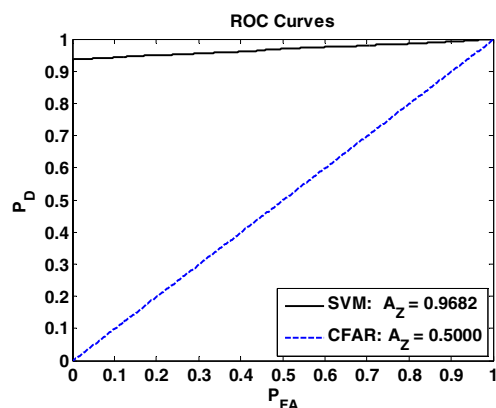


Figure 6. ROC Curves for experiment 5 (SNR = -25 dB).

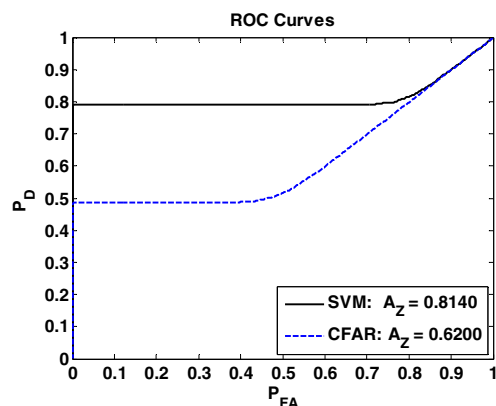


Figure 7. ROC Curves for experiment 6 (SNR varies from -25 to 10 dB).

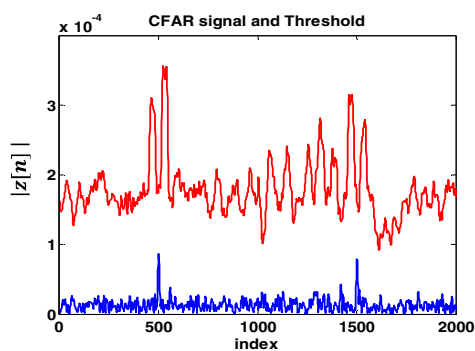


Figure 8. Example of signal and threshold values for experiment 5 for CFAR. The threshold is the upper curve. Targets are located at approximately indices  $n=500$  and  $1500$ .

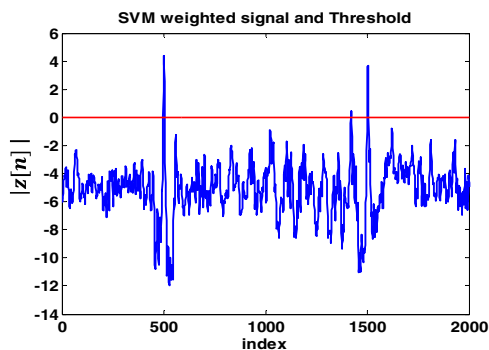


Figure 9. Example of signal and threshold values for experiment 5 for L-SVM method. The threshold is constant at zero. Note a false alarm just before index  $n=1500$ . Targets are located at approximately  $n=500$  and  $1500$ .

## V. FUTURE WORK

Future work includes analysis of other types of SVMs, such as nonlinear SVMs. Targets appearing in the leading or lagging windows can severely affect CFAR performance. Scenarios with multiple targets, such as a larger target with a smaller target nearby, and multiple targets will be studied. Targets using Doppler waveforms and multiple pulses will be studied. This study assumed interference was Gaussian noise in the I and Q channels. Cases with strong clutter returns (i.e. non-Gaussian noise) will be examined. Finally, a proof that the L-SVM method is a CFAR processor (that is, the false alarm rate is independent of the interference power) is needed.

## REFERENCES

- [1] M. A. Richards, Fundamentals of Radar Signal Processing, New York: McGraw Hill, 2005, pp. 347-383.
- [2] C. J. C. Burgess, A Tutorial on Support Vector Machines for Pattern Recognition, London: Kluwer Academic Publishers, pp. 1 – 43.
- [3] D. He and H. Leung, "CFAR Intrusion Detection method Based on Support Vector Machine Prediction," IEEE Intl. Conf. on Comp. Intell. for Meas. Systems and Intell., 14 Jul 2004, pp. 10-15.
- [4] G. P. Noone, "Radar pulse classification using support vector machines," Wrkshp. on the Appl. of Radio Sci., Natl. Comm. for Radio Sci., URSI Commission C, 27 – 29 April, 2000.
- [5] Y. Tang, X. Luo, and Z. Yang, "Ocean Clutter Suppression using support vector machines," IEEE Wkshp. on Machine Learning for Sig. Proc., pp. 559 – 568.
- [6] J. Guan, N. Liu, J. Zhang, and J. Song, "Multifractal correlation characteristic for radar detecting low-observable target in sea clutter," Signal Proc., Vol. 90, Jul. 2009, pp. 523-535.
- [7] A. Elridy, "Pulse Doppler radar target recognition using a two-stage SVM Procedure," IEEE Trans. Aero. And Elec. Syst., Vol. 47, No. 2, April 2011, pp. 1450 – 1457.
- [8] R.-E. Fan, K.-W. Chang, C.-J. Hsieh, X.-R. Wang, and C.-J. Lin, "LIBLINEAR: A library for large linear classification," *Jrnl. Machine Learn. Res.*, Vol. 9, August 2008, pp. 1871 – 1874.
- [9] C.-C. Chang and C.-J. Lin, "LIBSVM : a library for support vector machines," *ACM Trans. on Intelligent Systems and Tech.*, 2:27:1–27:27, 2011. Available: <http://www.csie.ntu.edu.tw/~cjlin/libsvm>
- [10] R. O. Duda, P. E. Hart, and D. G. Stork, Pattern Classification, New York: Wiley Interscience, 2001, pp. 48 – 5.